OPTICAL DIAGNOSTICS OF THE CYCLIC VARIATION IN THE KERNEL DEVELOPMENT AND ABNORMAL COMBUSTION: SI BOOSTED ENGINE

Jose Manuel Gallardo-Ruiz

E.T.S. Ingenieros Industriales, University of Malaga
Dr. Ortiz Ramos s/n, 29071 Málaga, Spain
e-mail: josemgallardo@uma.es

Rémi Ballais

SUPMÉCA/LISMMA-Paris, School of Mechanical and Manufacturing Engineering
3 rue Fernand Hainaut - 93407 Saint-Ouen Cedex, France
e-mail: remi.ballais@supmeca.fr

Simona Silvia Merola, Paolo Sementa, Cinzia Tornatore

Istituto Motori – CNR
via G. Marconi, 8 – 80125 Napoli (Italy)
e-mail: s.merola@im.cnr.it, c.tornatore@im.cnr.it, p.sementa@im.cnr.it

Abstract

The combustion stability of a spark ignition engine significantly influences its performances. The cyclic variation is generally evaluated by the fluctuation of in-cylinder peak pressure which changes in both magnitude and position measured from TDC. In this work the cyclic variation of combustion process were analysed as function of crank angles. The different SI engine process phases were investigated. The pressure related data were correlated with cycle resolved visualization measurements. The cycle resolved digital imaging was applied to follow the kernel inception and growth and to study the flame front propagation until the exhaust phase. A custom numerical post-detection procedure was applied to correlate the optical data from the integral luminous signal measured in the combustion chamber with the pressure related parameters .The flame kernel and the abnormal combustion due to the fuel deposits burning resulted particular relevant for the cycle-to-cycle variations. Optical measurements outlined better than pressure related analysis the role of the early and final stages of the combustion process.

The experiments were performed in a 400 cm3 single cylinder, port fuel injection, four-stroke spark ignition engine. The engine was optical accessible with the same geometrical parameters as a 1600 cm^3 passenger car engine. The head and the injection system of a commercial engine mounted on a passenger car were used. Standard EURO IV gasoline was used.

Keywords*: optical diagnostics; cycle-to-cycle variation; flame kernel; abnormal combustion; SI boosted engine*

1. Introduction

In order to reduce the emission levels and to improve the engine performance, the cyclic variation control and reduction is important step. Nowadays, the peak of the in-cylinder pressure is commonly used to control of the SI engine combustion. Just few cycles burn like the optimum cycle. This occurrence produces a loss of efficiency. The detailed understanding of the thermo-fluid dynamic phenomena that occur in the spark ignition engine process allows knowing the effective weight of the different combustion phases. The relevance of the early flame stages on the SI combustion is well known by literature [1]. The flame kernel inception and growth depend on some factors like the local air/fuel ratio, the mixture motion, the exhaust gas concentrations in the

spark plug gap at the ignition and the local temperature of the mixture next to the spark. A quantitative evaluation of the flame kernel phase on the cycle-to-cycle variation can be a useful parameter to control and optimize the spark ignition engines [2, 3]. To this target, in this work the cyclic variation was studied. Two approaches were considered: the first one was based on pressure related parameters and the second on optical measurements. Both the methodologies were cycle-resolved. Pressure data furnish immediate but global information about the engine combustion. On the other hand, they do not allow to locally investigating the spark ignited flame in the combustion chamber. A balanced synergy between optical and pressure related data is the optimal tool for the best understanding of SI combustion process including the cycle to cycle variation [4].

2. Experimental apparatus

Experiments were carried out in a 399 cm^3 single cylinder PFI SI four-stroke engine. The engine was equipped with the head and injection system of a four cylinders commercial engine mounted on a 1600 cm^3 passenger car. The boosting device consisted of an external compressed air system with a tank of 720 litres. It allowed the control of the intake air pressure in a range of 1000-2000 mbar and of the temperature in a range of 290-340 K. The engine bore was 79 mm, the stroke was 81.3 mm, the connecting road was 143 mm and the compression ratio was 10. The engine had four valves and a pent-roof combustion chamber, with the spark plug centrally located. The exhaust valves opening occurred at 140 CAD ATDC. A pressure transducer was flush-installed in the region between intake-exhaust valves at the side of the spark plug to perform in-cylinder pressure measurements in real-time, without changing the original compression ratio. The elongated piston was optically accessible through a flat quartz window (ϕ = 57 mm). Aluminium enhanced UV 45° mirror was placed in the cylinder at the bottom of the piston. The elongated piston was self-lubricated by Teflon-bronze composite piston rings in the optical section to avoid having oil on the quartz window. A special lube oil and coolant conditioning unit for transparent single cylinder engine application was used. The engine was fuelled with Euro IV gasoline.

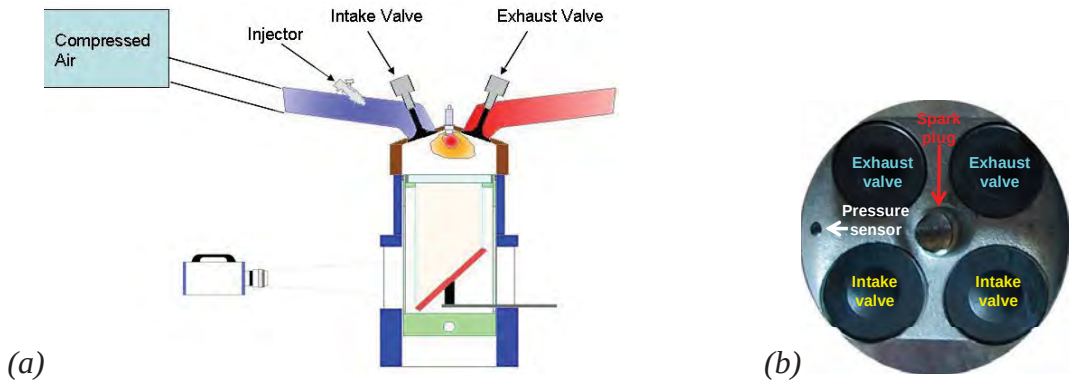

Fig. 1. (a) Optical investigations experimental apparatus and (b) bottom field of view of the combustion chamber

The luminosity produced by the combustion process passed through the quartz window and it reached the 45° inclined UV-visible mirror where it was reflected towards the optical detection assembly. This was constituted by an 8-bit 512 x 512 pixel CMOS camera (Optronis CamRecord 5000) equipped with a 50 mm focal Nikon lens. The camera spectral range extended from 380 nm to 780 nm. A camera region of interest was selected (400 x 400 pixel) to obtain the best match between spatial and temporal resolution. This optical assessment allowed a spatial resolution around 0.186 mm/pixel. The exposure time was fixed at 25 μs that corresponds to about 0.3 CAD at an engine speed of 2000 rpm and the dwell time between two consecutives images was around 1.85 CAD. Thus the camera frame rate was 6470 fps. Fig. 1 shows the experimental apparatus for the optical investigations with the bottom field of view of the combustion chamber.

Crank-angle-degree resolved data were acquired using an AVL IndiModul 621 coupled to a shaft encoder. The shaft encoder produced an output pulse signal every 0.05 CAD. The pulse provided a common signal to synchronize the time and CAD clocked data. Data were collected using IndiCom software. In this work 0.1 crank angle resolution with a known reference to top-dead-centre of the cylinder was fixed. The IndiModul furnished cylinder pressure traces as well as heat-release curves and combustion statistics at near-real time speed as the engine was operated in the test cell. The in-cylinder pressure and the related parameters were evaluated on an individual cycle basis and/or averaged on 400 cycles. All the results presented in this work were carried out at an engine speed of 2000 rpm and at wide open throttle. The fuel was injected at an absolute pressure of 1.4 bar in the intake valve manifold (0.4 bar boosting). The duration of injection was fixed at 140 CAD that corresponded to a stoichiometric air-fuel ratio, as measured by the exhaust lambda sensor. The start of injection was set at 130 CAD ATDC, corresponding to the phasing of the reference commercial engine for the same engine speed and load. In this case the intake valves were closed during the injection, impacting fuel against the backside of the intake valve, which was heated by the previous cycle of combustion. The contact of the fuel with the backside of the intake valve allowed the vaporization the fuel. The spark timing was fixed at 14 CAD BTDC to operate at maximum brake torque before the knock limit [5]. To reduce the effects of the initial conditions, the engine was preheated by the conditioning unit, and it was maintained in motored condition by an electrical engine until the temperature reached 60ºC. After the warm-up, the engine worked in fired conditions for 300 consecutive cycles. Optical acquisitions were carried out in the last 35 cycles. Then the engine returned in motored condition for 100 cycles. This phase allowed checking an eventual change in the thermal and fluid-dynamic status of the engine from the beginning of the measurements. During all motored and fired cycles, engine parameters and pressure signals were measured. The test procedure is sketched in Fig. 2.

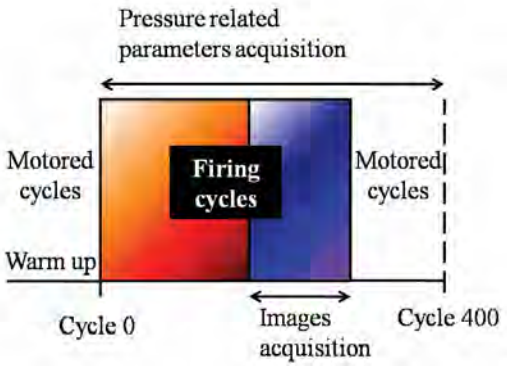

Fig. 2. Sketch of the test procedure

The pressure data were post-processed using a numerical procedure developed in Labview of National Instruments environment. The procedure evaluated the maximum pressure value and the related CAD for each engine cycle. The same procedure was applied for the heat release values. A retrieving procedure of the optical data was realized to process each image. The optical diagnostics consisted in capturing and post-processing the global luminosity emitted in the combustion chamber in the visible range. The external spurious light determined some interferences and ghosts that influenced the image quality. The spurious light was reflected on the skirt creating on the images a luminous annulus around the limits of the combustion chamber, and it has been considered as noise. In order to eliminate these interferences, a reference image was used as background and then it was subtracted from the analyzed images. After this step a region of interest was selected. This operation allowed eliminating the luminous noise due to the reflections on the piston wall of the combustion process radiation. The reference image was detected at the CAD before the spark ignition timing for each engine cycle. Each image was converted in a numerical matrix. The global luminosity was calculated by the integration of

luminosity from each pixel. The mean integral signals were evaluated dividing the total intensity by the pixel number in the selected region of interest. Thus the intensities resulted in 8-bit scale. This procedure allowed comparing different cycles and experiments without the influence of the optical setup parameters (exposure time, gate etc.). The rate of luminosity was calculated as a first order, backward finite differences technique of the luminosity. The luminous signals and the pressure related values were correlated following a statistical approach. The coefficient of variation COV and coefficient of correlation R were calculated [3, 6].

$$COV(\%) = \frac{\sigma}{\mu}, \qquad R(X,Y) = \frac{Co\,\mathrm{var}(X,Y)}{\sigma(X)\sigma(Y)} \quad \text{with} \quad Co\,\mathrm{var}(X,Y) = \sum_{i=1}^{n} \frac{(X_i - \overline{X})(Y_i - \overline{Y})}{n-1},$$

$\overline{X}$ is the mean value of X and $\sigma(X)$ is the standard deviation of X.

For pressure data the COV at maximum values was evaluated. The COV at the pressure peak is a standard parameter to estimate the engine cycle variability. This value is suitable for the quick evaluation of the engine combustion efficiency; on the other hand it doesn't furnish detailed information to understand the complex phenomena correlated to the cycle-to-cycle variation. To better investigate these phenomena, crank angle resolved COV was calculated for both the optical and pressure data.

3. Results and discussion

Figure 3 reports the cycle resolved flame propagation detected in the combustion chamber for a selected engine cycle. The evidence of the spark ignition occurred around 14 CAD BTDC and it was represented by a luminous arc near the spark plug. Spark plasma emission persisted until about 11 CAD BTDC. After this time the flame kernel was observable, even if its luminosity was very lower than the spark. The kernel resulted asymmetrical with negative curvatures on the intake valves side. Moreover, the flame front propagation was faster towards the exhaust valves. The flame reached the combustion chamber walls around 8 CAD ATDC (images 2-8). Moreover, several bright spots were detected in the burned gas from the first times of the combustion process.

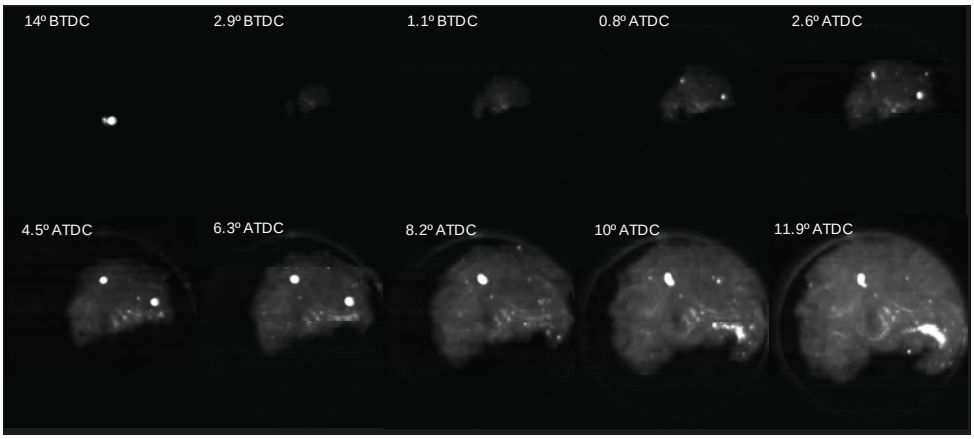

Fig. 3. Cycle-resolved visualization from the spark ignition evidence to the match of the flame front with the combustion chamber walls

The asymmetry and the bright spots were both due to the presence of liquid fuel deposits in the combustion chamber. It is known that in a PFI engine a part of the injected fuel is deposited on the intake manifold surfaces and forms a layer of liquid film on the valve and port surfaces [7, 8]. The film needs to be re-atomized by the shearing airflow as the intake valves open. If these fuel layers are not well atomized they enter the cylinder as drops and ligaments [9-11]. The fuel deposits were drawn by gravity on the valve head where they remained as film due to the surface tension.

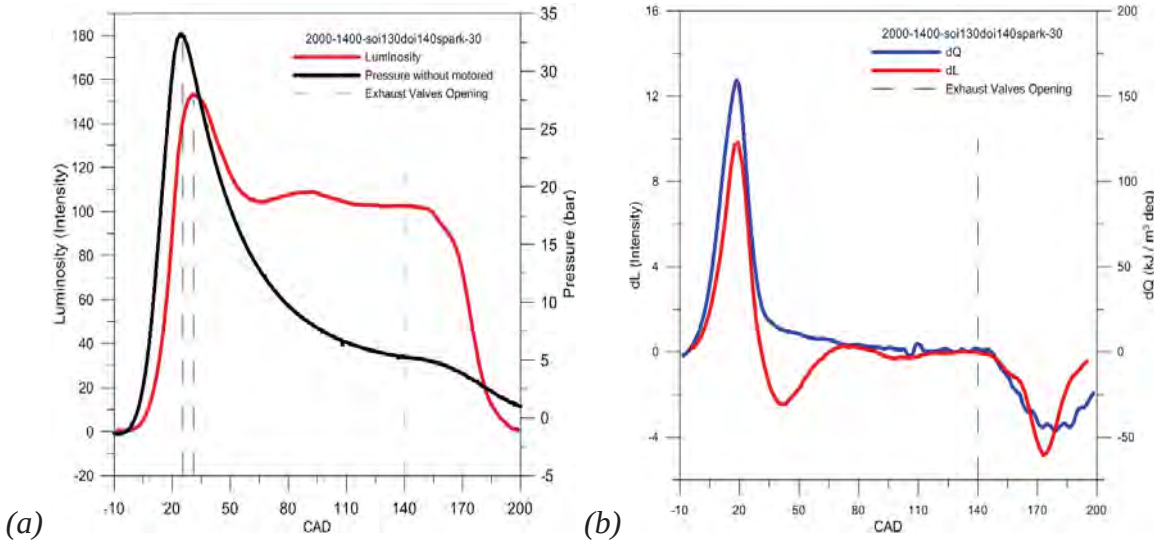

Fig. 4. Comparison between the combustion pressure signal and the integral luminosity (a) and between the rate of heat release and of the integral luminosity (b)

Successively, the fuel film squeezing determined the deposition of rich-fuel zones around the intake valves. When the flame propagated in the normal direction to an area with equivalence ratio gradient, each part of the front evolves in a field with varying fuel concentration. This induced variation of the propagation speed along the flame front and an increase in flame wrinkling. This is the reason of the flame front asymmetry. Moreover, the strip atomization of a part of the fuel squeezed film caused the depositing of the fuel on the cylinder walls and on the piston surface, as a sort of drops. These fuel deposits created fuel-rich zones that ignited when reached by the normal flame front causing the bright spots. This is particularly intensified during cold operation, when evaporation is low. The presence of fuel deposits as squeezed film or impinged droplets had direct effect on the cyclic variability and flame stability [12, 13].

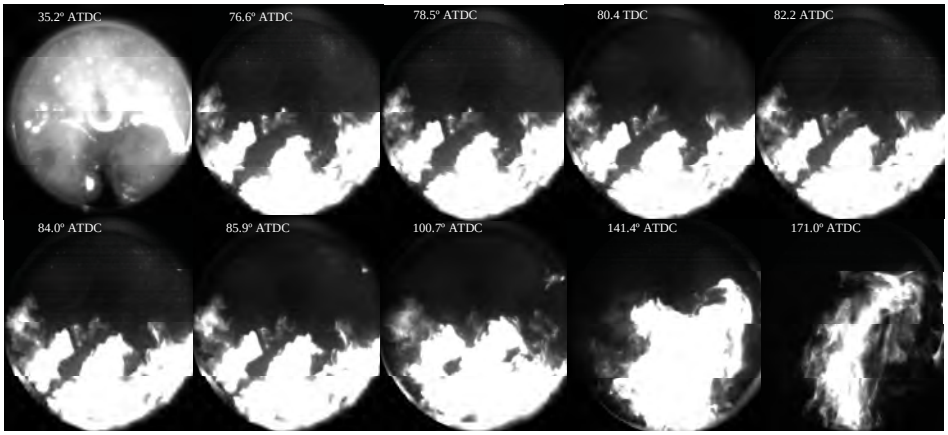

Fig. 5. Cycle-resolved visualization of the late combustion phase

The pressure signal after the subtraction of the motored one was considered for each engine cycle and it was compared with the integral luminosity measured by CMOS during the combustion process. Moreover a comparison between the rate of heat release and of the integral luminosity rate was performed too. The results for the engine cycle of Fig. 3 are shown in Fig. 4. From the spark ignition to the maximum values (near 30 CAD ATDC) the luminosity and pressure and their related signals showed the same trends. This occurred as consequence of the chemical reactions which occurred in the first times of the combustion process. The exothermic and irradiative nature

of these reactions promoted the pressure and luminosity increasing. After 30° ATDC, the combustion pressure and luminous intensity had a similar trend, they decreased for about 35 CAD. Around 65° ATDC a new increase in the luminosity was detected. This was due to the fuel deposits burning in the combustion chamber. In fact, as previously discussed, the port fuel injection created fuel-rich deposits near the intake valves that ignited when the normal flame front reached them [14, 15]. This induced the inception of diffusion-controlled flames that persisted with high intensity still after the normal combustion event. A selection of the flame emission images detected in the late combustion phase is shown in Fig. 5. The intake valves outlines are delineated by the fuel deposits burning. After 50° ATDC, the expansion piston movement determined the normal combustion was diminishing and the diffusion-controlled flames spreading out. As a consequence, the integral luminosity increased, aided also to the line of sight nature of digital imaging, while the in-cylinder pressure decreased. Thus, in agreement with literature [8, 16], the diffusion controlled flames didn't contribute to the engine work and they very poorly influenced the pressure signal. In fact, the fuel deposits burning near valves are surface diffusion flames that warmed up the nearby in-cylinder gas by thermal diffusion. This fact increased the pressure much slower than the reduction of pressure produced by the movement of the piston during the expansion stroke. The diffusion-controlled flames persisted well after the normal combustion event and they were still detectable at the Exhaust Valves Opening (EVO). At this time, optical and pressure signals decreased. This was well observable by heat release and luminosity rate of Fig. 4b.

The early stages of combustion strongly influence the later flame development; the flame kernel inception and growth can have significant relevance in the combustion efficiency variability [1, 2, 6]. Fig. 6 shows flame images measured at 4.5 CAD ATDC on 10 of 25 cycle consecutive cycles. At this time, the flame kernel was formed and the radial-like shape of the flame outline can be observed. The bright spots due to the burning of the fuel deposits on the piston surfaces were detected for each cycle. The cyclic variation of the flame is evident.

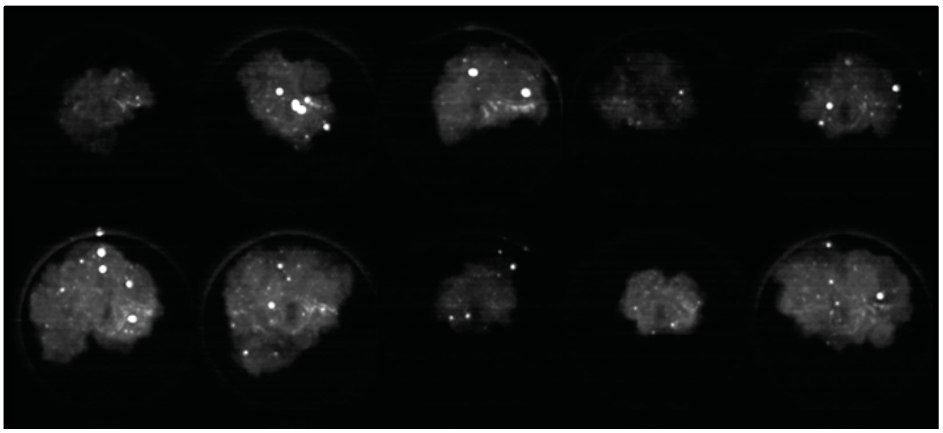

Fig. 6. Flame kernel detected on 10 consecutive cycles at 4.5 CAD ATDC

Conventional analysis of pressure signals allow to calculate the COV from pressure peak, it is equal to 8.41% with a correlation coefficient R^2=0.92. On the other hand the COV evolution versus CAD evaluated for the pressure in Figure 7a showed a wide range of values. The pressure COV spreads from 0.3% to 15.8 %. From 360 CAD BTDC up to 130 CAD BTDC, the COV values are high with strong noise and they show a weak decreasing. The COV relevance is related to the low in-cylinder pressure. After the intake valve closing, the COV reaches a first minimum value. Around 130 CAD BTDC the intake valves start closing and COV decreases faster to a first local minimum. In agreement with literature, until this minimum, the COV depends only on the average pressure according the relation: $COV=\alpha/P^{0.5}$ with, P the average pressure, and α a constant. α depends only on the experimental apparatus and it is not related to engine operating

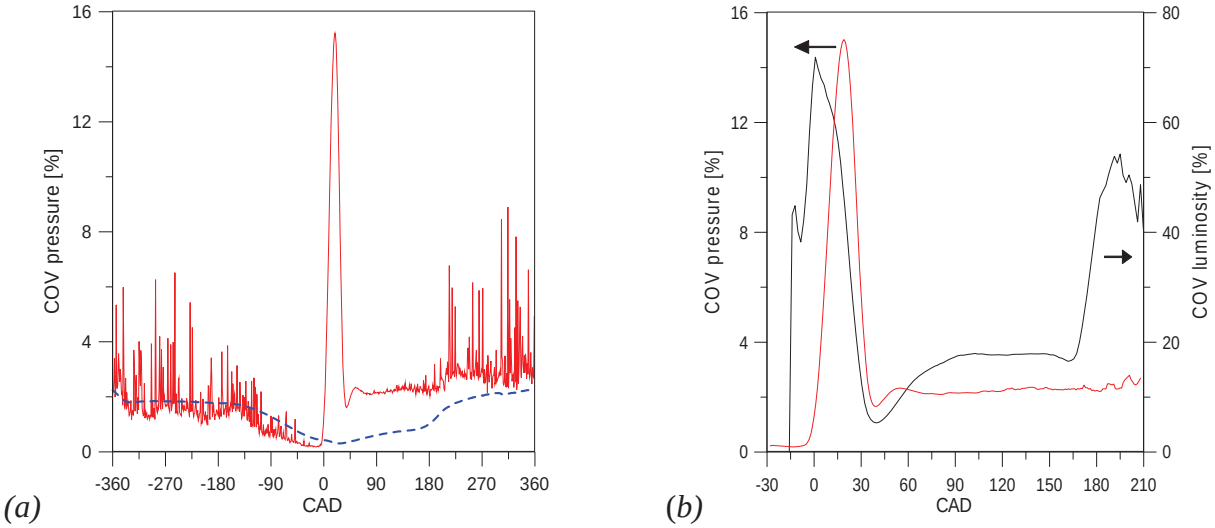

Fig. 7. COV of the in-cylinder pressure versus crank angle (a) and COV of the in-cylinder pressure and luminosity versus crank angle in the range from 30 CAD BTDC to 210 CAD ATDC (b)

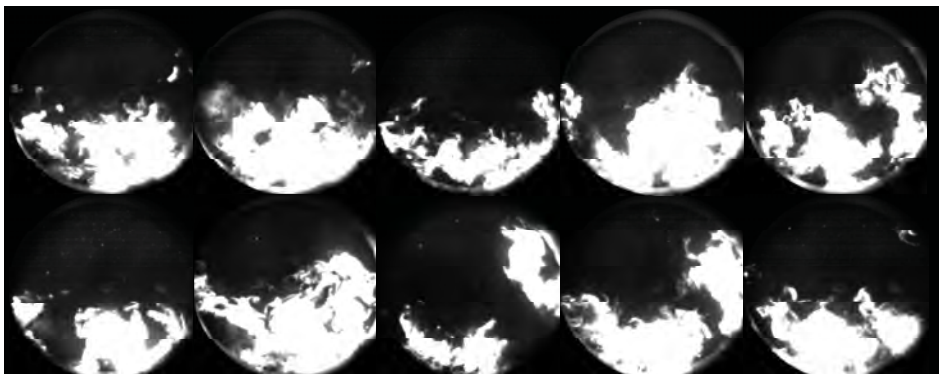

Fig. 8. Late flame detected on 10 consecutive cycles at 100 CAD ATDC

conditions. Thus α is the same both in the motored and fired cycles and it represents the noise level of the engine. In this work, $\alpha \cong 2$. After the first minimum a sharp COV increasing is observed. It starts in correspondence of the normal combustion inception and it rises until to the absolute COV maximum. This demonstrates the high COV value already from the first times. The COV maximum occurs at the maximum of the heat release rate (Fig. 5b). After this time, a fast COV decrease until a second local minimum point is observed. This behaviour is caused by the progressive reduction of the spark ignited combustion weight if compared to the increasing of the combustion chamber volume due to the piston motion. The second COV minimum cannot be used as marker of the normal combustion end because another COV local maximum closed to it can be measured. This is due to the abnormal combustion caused by the fuel deposits burning. Around 90 CAD BTDC, the COV pressure curve is again dominated by the piston expansion and doesn't longer follow the abnormal combustion phenomenon. Then the COV evolves to a plateau that corresponds to the exhaust phase. Around 200 CAD ATDC a little increasing in the COV is evaluated. This occurs because COV is leaded by the expansion volume change due to the low pressure values. Anyway the COV values are higher in the motored phase and noise is higher. This occurs because of the in-cylinder pressure is higher than the motored one at the same CADs. COV from luminosity shows a similar evolution but a different trend in the first times of the spark ignition combustion than COV from pressure (Fig. 7b). Thus it allows obtaining more information than to pressure data. COV from luminous signals is strongly influenced by the early stages of the combustion process and by the late combustion in the exhaust phase. It shows a first local

maximum in at the kernel flame formation. This result quantifies the cyclic variability of the kernel. The pressure data analysis does not give the right weight to the early stages of the combustion. In this sense the optical measurements are a powerful tool for the study of the processes in spark ignition engines. From spark ignition timing to about TDC, the COV from luminosity sharply increases with a first local maximum at about 13 CAD BTDC due to spark ignition plasma emission. The strong luminous COV rising is principally due to the high variability of the flame kernel. At 4.5 CAD ATDC, COV from pressure is about 4%; on the other hand in the images of Figure 6 the flame area shows a strong variability that is well evaluated by COV from luminosity higher than 60%. These instabilities can result negligible if evaluated by the pressure signal. From TDC to 30 CAD ATDC, the spark ignition flame occupies the whole combustion chamber optical section and the expansion phase occurs. As a consequence, the luminous signal fluctuations are not significant. COV from luminosity decreases with a similar trend than COV from pressure and they reach together the minimum. Also for the luminous signal, this minimum cannot mark the normal combustion event end. The inception of the diffusion controlled flames induces a progressive and smooth increasing in the COV from luminosity. The strong cyclic variability of the abnormal combustion phase is evident in Figure 8 that shows the images acquired at 100 CAD ATDC for 10 consecutive cycles. The cycle-to-cycle variation of diffusion controlled flame in terms of spatial distribution is clear. Around 160 CAD ATDC the exhaust valves are opening and the COV from luminosity quickly rises up. It reaches a maximum when the opening is complete. The reduction of diffusive flames due to fuel deposits burning is a fundamental step for reducing the fuel consumption, the exhaust emissions and also the life expectancy of the engines. In fact, the temperatures reached when these flames occur are very high and the mechanic parts are strongly stressed.

4. Conclusions

Pressure related parameters and cycle resolved optical data were correlated to better understand some of the phenomena that occur in the spark ignition engine process. Particular interest in the early stages of combustion and in its late phase was paid. Pressure related methodologies are powerful tool for the spark ignition engine real-time analysis. On the other hand, pressure data global information about the engine combustion and they do not allow a local analysis in the combustion chamber. Thus the relevance of the flame kernel inception and growth on the cycle-to-cycle variation was emphasized only by the optical measurements. Similar results were obtained for the abnormal combustion due to the fuel deposits burning in the combustion chamber. The quantitative evaluation of the flame kernel phase and the abnormal combustion weight on the cycle-to-cycle variation can be a useful parameter to control and optimize the SI engines.

References

[1] Mansour, M., Peters, N., Schrader, L. U., *Experimental study of turbulent flame kernel propagation*, Experimental Thermal and Fluid Science, Vol. 32, pp. 1396-1404, 2008.
[2] Lee, K. H., Kim, K., *Influence of initial combustion in SI engine on following combustion stage and cycle-by-cycle variations in combustion process*, Int. J. of Automotive Tech. Vol. 2 (1), pp. 25-31, 2001.
[3] Galloni, E., *Analyses about parameters that effect cyclic variation in a spark ignition engine*, Applied Thermal Engineering, Vol. 29, pp. 1131-1137, 2009.
[4] Drake, M., Haworth, D., *Advanced gasoline engine development using optical diagnostics and numerical modelling*, Proceedings of the Combustion Institute, Vol. 31 (1), pp. 99-124, 2007.
[5] Zhu, G. G., Daniels, C. H., Winkelman, J., *MBT timing detection and its closed-loop control using in-cylinder pressure signal*, SAE Technical Paper n, 2003-01-3266, 2003.

[6] Zervas, E., *Correlations between cycle-to-cycle variations and combustion parameters of a spark ignition engine,* Applied Thermal Engineering, Vol. 24 (n.14-15), pp. 2073-2081, 2004.
[7] Costanzo, V. S., Heywood, J. B., *Mixture Preparation Mechanisms in a Port Fuel Injected Engine*, SAE Technical Paper n, 2005-01-2080, 2005.
[8] Nogi, T., Ohyama, Y., Yamauchi, T., Kuroiwa, H., *Mixture Formation of Fuel Injection Systems in Gasoline Engines*, SAE Technical Paper n. 880558, 1988.
[9] Henein, N. A., Tagomori, M. K., *Cold-start hydrocarbon emissions in port-injected gasoline engines*, Progress in Energy and Combustion Science, Vol. 25, pp. 563-593, 1999.
[10] Behnia, M., Milton, B. E., *Fundamentals of fuel film formation and motion in SI engine induction systems*, Energy Conversion and Management, Vol. 42 (15-17), pp. 1751-1768, 2001.
[11] Gold, M. R., Arcoumanis, C., Whitelaw, J. H., Gaade, J., Wallace, S., *Mixture Preparation Strategies in an Optical Four-Valve Port-Injected Gasoline Engine,* Int. J. Engine Research, Vol. 1 (1), pp. 41-56, 2000.
[12] Bianco, Y., Cheng, W., Heywood, J., *The Effects of Initial Flame Kernel conditions on Flame Development in SI Engines.* SAE Technical Paper n. 912402, 1992.
[13] Witze, P., Hall, M., Bennet, M., *Cycle-resolved Measurements of Flame Kernel Growth and Motion Correlated with Combustion Duration*, SAE Technical Paper n. 900023, 1990.
[14] Zhu, G. S., Reitz, R. D., Xin, J., Takabayashi, T. *Modelling Characteristics of Gasoline Wall Films in the Intake Port of Port Fuel Injection Engines,* Int. J. of Engine Research, Vol. 2 (4), pp. 231-248, 2001.
[15] Merola, S. S., Sementa, P., Tornatore, C., Vaglieco, B. M., *Effect of Injection Phasing on Valves and Chamber Fuel Deposition Burning in a PFI Boosted Spark-Ignition Engine*, SAE Technical Paper n. 2008-01-0428, 2008.
[16] Witze, P. O., Green, R. M., *LIF and Flame-Emission Imaging of Liquid Fuel Films and Pool Fires in an SI Engine During a Simulated Cold Start.* SAE Technical Paper n. 970866, 1997.